Towards Environmental Monitoring with Mobile Robots

Marco Trincavelli, Matteo Reggente, Silvia Coradeschi, Amy Loutfi, Hiroshi Ishida and Achim J. Lilienthal

Abstract— In this paper we present initial experiments towards environmental monitoring with a mobile platform. A prototype of a pollution monitoring robot was set up which measures the gas distribution using an "electronic nose" and provides three dimensional wind measurements using an ultrasonic anemometer. We describe the design of the robot and the experimental setup used to run trials under varying environmental conditions. We then present the results of the gas distribution mapping. The trials which were carried out in three uncontrolled environments with very different properties: an enclosed indoor area, a part of a long corridor with open ends and a high ceiling, and an outdoor scenario are presented and discussed.

I. INTRODUCTION

We are embarking on a new era of environmental awareness and consequently witnessing a number of new legislations, new products and recommendations being implemented to improve air quality particularly in urban environments. On a European level, for example, the framework directive 1996/62/EC on ambient air quality assessment and management lead to the specification of limit values for a number of pollutants.

As important as these new implementations are, we need to be able to correctly validate and confirm the effect of these new policies on the environment in order to effectively judge their impact. Currently, many monitoring systems consist of a static network of sensors which are distributed at key locations. These systems typically monitor pollution levels at a rather large scale. A natural development of this monitoring strategy is to refine the monitoring scale and also use mobile sensors to collect information about air quality and the environmental conditions as it is needed. Mobile robotics can make a significant contribution in this area by providing robots that autonomously monitor different environments, cooperate with other systems and collect data. This is particularly appealing in a scenario where mobile robots are already available at the particular site. The mobile robot platform introduced in this paper is a prototype that implements the monitoring aspect of a cleaning and pollution monitoring robot that is developed for the EU project "DustBot" [1]. An additional application area is robots exploring hazardous environments for instance in rescue scenarios.

Marco Trincavelli, Matteo Reggente, Amy Loutfi, Silvia Coradeschi and Achim J. Lilienthal are with the AASS Research Centre, Örebro University, SE-701 82 Örebro, Sweden. E-mail: `firstname.lastname@aass.oru.se` for A. Lilienthal use E-mail: `achim@lilienthals.de`

Hiroshi Ishida is with the Department of Mechanical Systems Engineering, Tokyo University of Agriculture & Technology, Tokyo, Japan. E-mail: `h_ishida@cc.tuat.ac.jp`

In this paper we describe the design of a pollution monitoring robot including the selection and set-up of sensors for measuring gas concentration, wind, temperature and humidity. In addition, we describe the experimental set-up that enabled us to run monitoring trials under largely varying environmental conditions (indoors and outdoors) and report our experience from these experiments. An explicit focus is on the gas distribution modeling problem and the interrelation between the observed wind field and gas distribution.

Gas distribution mapping has been previously addressed in smaller and controlled areas [2], [3], [4], including wind tunnels [5]. Apart from the description of set-up and operation of the pollution monitoring robot, a major contribution of this paper is the extension of gas distribution mapping to larger and less controlled environments – an important development for real applications.

We consider three different scenarios, an enclosed room (later called "microscope room", larger but otherwise similar to the environment considered in previous publications on gas distribution mapping), an open area that is part of a larger corridor where people passed by, doors and windows were opened and closed during the experiment (similar to the corridor scenario considered in [6]), and an outdoor scenario with accordingly much higher airflow and changes in temperature and humidity. To our knowledge, gas distribution mapping with mobile robots has never been addressed before under outdoor conditions. A further contribution resides in the observation of the correlation of sensor data between the different sensor modalities throughout both large indoor and outdoor environments. This is particularly critical in light of the difficulty of ground truth validation which is a general problem in the field of mobile olfaction.

The rest of this paper is organized as follows. After a review on related works (Section II) and a description of the set-up of our pollution monitoring robot (Section III), the gas distribution mapping algorithm used in this work is described in Section IV, including a discussion of the particular issues of gas distribution mapping. Then, the experimental setup is detailed in Section V, followed by a discussion of the results in Section VI. The paper ends with conclusions and a discussion of possible extensions of the presented system.

II. RELATED WORK

Monitoring of urban environments is typically done by stationary monitoring stations, typically several stations in a city [7]. However, under some conditions of weather and terrain, pollutants are accumulated in a confined area, e.g. in street canyons, and create local but intense pollution. The need for refining the monitoring scale motivated the

development of small inexpensive gas sensors for air pollution monitoring, which enables sensor networks with a large number of sensors deployed in the fields [8]. A mobile robot equipped with such sensors can be used for collecting gas concentration data at various locations and generating a gas distribution map of the given environment [2], [3], [4], [5]. However, a difficulty lies in the fluctuating nature of the gas distribution.

In general environments, advective flow dominates gas dispersal compare to slow molecular diffusion. Since the airflow we encounter is almost always turbulent, the gas distribution becomes patchy and meandering [9]. One way to work around is to measure the gas concentration for at least several minutes at each location to obtain a statistically significant measure, e.g. time average [2], [5]. To obtain a map of good quality in shorter time, model equations representing turbulent diffusion process and/or resultant gas distributions can be used to estimate the gas dispersal in the whole area from a limited number of measurement points [4]. However, a uniform airflow field has to be assumed in those methods, and the experimental validations were mostly done in small controlled areas in which this assumption could reasonably be made. On the other hand, we used kernel-based extrapolation for gas distribution mapping [3], [10]. As a model-free method, this approach does not assume a pre-defined functional form of the gas distribution and is therefore not restricted to specific situations but yet provides a way to integrate the measurements performed over time and extrapolate on the sparse measurement points.

Autonomous search for the location of a gas source is another important subject for mobile robots equipped with "electronic noses". Various hardware and software setups are proposed so far, and their details can be found in the review [11]. Most of the robots use gas concentration gradient and airflow direction to track gas plumes to their source. However, the experimental demonstrations were mostly given again in small controlled environments. In most of the cases, uniform strong airflow fields were artificially created. Otherwise, small areas in larger rooms were carefully chosen to have constant airflow. Consequently, the next challenge is to achieve successful gas source localization in larger and uncontrolled environments, e.g. under outdoor conditions. The data we are collecting will serve as the basis for devising and evaluating the appropriate gas source localization algorithms and the hardware setups.

III. THE POLLUTION MONITORING ROBOT

Apart from a laser range scanner (SICK LMS 200) used for localization, the robot used in the experiments is equipped with an "electronic nose" and an anemometer. The "electronic nose" comprises six gas sensors enclosed in an aluminum tube. This tube is horizontally mounted at the front side of the robot at a height of 34 cm (see Fig. 1). The "electronic nose" is actively ventilated through a fan that creates a constant airflow towards the gas sensors. Thus, it lowers the effect of external airflow and the movement of the robot on the sensor response and guarantees a continuous
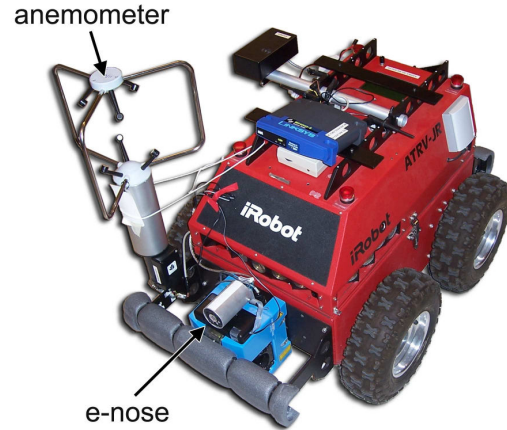

Fig. 1. The pollution monitoring robot "Rasmus" equipped with an "electronic nose" ("e-nose") and an anemometer.

exchange of gas in situations with very low external airflow. A brief description of the gas sensors used in the "electronic nose" is given in Table I. Different types of sensors were chosen so that the "electronic nose" can respond to a variety of gases. In this work, however, we consider the case of a single gas source only.

The ultrasonic anemometer used to measure the airflow is a Young 81000 with a range from 2 cm/s up to 40 m/s with a resolution of 1 cm/s. We know from experience in indoor gas-distribution measurements that the airflow field and the resultant gas distribution can be essentially three dimensional in some environments. The placement of the anemometer had to be a compromise between the desire to measure the airflow as close to the gas sensors and as undisturbed as possible. It was finally placed above the top of the robot in order to minimize the influence of the fan of the "electronic nose", the advective flow created by the heated metal oxide sensors, and the body of the robot itself.

Model	Gases Detected	Quantity
Figaro TGS 2600	Hydrogen, Carbon Monoxide	2
Figaro TGS 2602	Ammonia, Hydrogen Sulfide, VOC (volatile organic compound)	1
Figaro TGS 2611	Methane	1
Figaro TGS 2620	Organic Solvents	1
Figaro TGS 4161	Carbon dioxide	1

TABLE I

GAS SENSORS USED IN THE "ELECTRONIC NOSE".

The robot software is based on the Player robot server [12], a control interface that simplifies access to standard robot sensors and actuators and provides implementations of standard algorithms. For the experiments in this paper, adaptive Monte Carlo localization (amcl driver), VFH+ obstacle avoidance (vfh driver) and the wavefront path planner (wavefront driver) were used for localization, local and global path planning. The localization module implemented

in the amcl driver uses the odometry and the laser scanner readings in order to localize the robot on a map provided to the algorithm at the startup. Compared to using a SLAM approach, this has the advantage that all experiments in a certain environment refer to the same coordinate system without subsequent alignment of the obtained maps and it also allows to specify the same robot trajectory for all the experiments. The output from the adaptive Monte Carlo localization module was used as the pose estimate x^t of the robot at time t.

IV. GAS DISTRIBUTION MAPPING

The general gas distribution mapping problem given the robot trajectory x^t and the gas sensor measurements z_{gas}^t can be put as to estimate the posterior probability distribution over gas distribution maps m_{gas}

$$p(m_{gas}|x^t, z_{gas}^t) \qquad (1)$$

given the robot trajectory x^t and the gas sensor measurements z_{gas}^t. Due to fundamental differences between range sensing with a laser scanner and gas sensing with metal oxide sensors (which are the most widely used gas sensors in mobile robotic applications) Bayesian estimation cannot be applied to the gas distribution mapping problem in the same way as to estimate an occupancy grid map.

The main differences are, first, that the sensor readings do not allow to derive the instantaneous concentration levels directly. Metal oxide gas sensors are known to recover slowly after the target gas is removed (15 to 70 seconds) and therefore perform temporal integration implicitly. Sensor readings can be comparatively high although the instantaneous concentration level is actually close to zero if a high gas concentration was sensed previously. In order to estimate the instantaneous concentration level from a sequence of sensor readings, one would need to model the interaction between the gas sensors and the (unobserved) times when the sensors were "hit" by patches of gas and also their respective (unobserved) strength. Second, a snapshot of the gas distribution at a given instant contains little information about the distribution at another time due to the chaotic nature of turbulent gas transport. Turbulence generally dominates the dispersal of gas. As a consequence, the instantaneous concentration field of a target gas released from a small static source is a chaotic distribution of intermittent patches with peak concentration values an order of magnitude higher compared to the time-averaged values [9]. Third, gas sensor measurements require direct interaction between the sensor surface and the analyte molecules. Only those molecules that reach the surface of the sensor within its integration time affect the response. Compared to typical range sensors such as sonar or a laser range scanner, the area about which gas sensors provide information is therefore comparatively small.

As a result, we instead consider the *time-averaged* gas distribution and approximate the expectation

$$p(m_{gas}^{av}|x^t, z_{gas}^t). \qquad (2)$$

using the Kernel-GDM algorithm [13]. The main idea is to interpret gas sensor measurements z_{gas}^t as noisy samples from a time-constant distribution assuming that the gas distribution in fact exhibits time-constant structures. It is important to note that the noise is caused by the large fluctuations of the instantaneous gas distribution while the electronic noise on individual gas sensor readings is negligible [14].

The Kernel-GDM method compensates for the small overlap between single measurements by convolving the sensor readings with a two-dimensional Gaussian kernel. The kernel can be seen as modelling the decreasing information content of a given measurement about the average concentration distribution at an increasing distance with respect to the point of measurement. Kernel-GDM has a notable analogy with the problem of estimating density functions using a Parzen window approach with a Gaussian kernel. However, when creating the gas distribution map, we do not sample from the gas distribution directly. It is therefore necessary to make the assumption that the trajectory of the robot (respectively, the trajectory of the sensors) roughly covers the available space. The Kernel-GDM method maintains two temporary grid maps obtained from spatial integration of the points of measurement convolved with the Gaussian kernel. One temporary grid map $M_{xz_{gas}}$ integrates the points of measurement weighted by the sensor measurements and the second temporary grid map M_x integrates the points of measurement without a weight assigned. The gas distribution m_{gas}^{av} is estimated from the grid map $M_{xz_{gas}}$ normalised to M_x, which corresponds to sampling from the (normalised) gas distribution if the sensor readings are considered as a measure of how many samples were drawn from the particular grid cell. Because of the normalisation to M_x, a perfectly even coverage of the inspected area is not required so that the robot trajectory not necessarily has to be customised for gas distribution mapping.

The Kernel-GDM method can cope to a certain degree with the temporal and spatial integration of successive readings that metal-oxide gas sensors perform implicitly. In order to obtain a faithful representation of gas distribution the robot's path needs to fulfill the requirement that the directional component of the distortion due to the "memory effect" is averaged out. This can be achieved approximately by random exploration or by using a predefined path where the robot passes each point in the trajectory equally often from opposite directions. If the trajectory of the robot fulfills this requirement and if sufficient time is given for the map to converge, the time-constant structures of the gas distribution will be represented faithfully in the gridmap - under the assumption, of course, that these time-constant structures really exist.

The algorithm introduces the kernel width σ as a selectable parameter, corresponding to the size of the region of extrapolation around each measurement. The value of σ has to be set large enough to obtain sufficient coverage according to the path of the robot. Conversely, this means that for a larger kernel width a faster convergence can be achieved while preserving less detail of the gas distribution

in the map. Consequently, the selected value of the kernel width σ represents a trade-off between the need for sufficient coverage and the aim to preserve fine details of the mapped structures. Parameter selection and the impact of sensor dynamics are discussed in more detail in [10].

V. EXPERIMENTAL SETUP

In the experiments, the robot followed a predefined sweeping trajectory covering the area of interest, using a fixed starting point. Along its path, the robot stopped at predefined positions (waypoints) and carried out a sequence of measurements on the spot for 10 s (outdoors) and 30 s (indoors). All the measurements were recorded at a frequency of 1 Hz. The reason for stopping the robot at each waypoint to collect wind measurements is due to the difficulty in compensating for the movement of the robot on the anemometer readings. This is particularly critical in indoor conditions with slight airflow. Also in order to compare different sensing strategies for air pollution monitoring, a sequence of sensor readings from periods where the robot was stopped will provide more reliable information about the average wind and concentration at the measurement point. Nonetheless, it is the ambition of future works to record all measurements while the robot is moving as a larger area can be covered.

The predefined sweeping motion was performed once in each directions and the robot was driven at a maximum speed of 5 cm/s in between the stops. For all experiments, the gas source used was a small cup filled with ethanol and it was possible that the robot could drive over the source. As previously mentioned, three different environments have been selected for the pollution monitoring experiments. The first set of experiments were carried out in an enclosed indoor area consisting of three rooms separated by protruding walls. The area covered by the path of the robot is approximately 14×6 m^2. This environment differs from the similar locations considered in previous publications on gas distribution mapping as there is very little exchange of air with the "outer world" and the gas distribution is actually monitored in the whole area, not only in a part of it. In this environment, the gas source was placed in the middle of the central room. A map of the laser scan readings is shown in Figure 4. The second location chosen was a section of a long corridor with open ends and a high ceiling. The area covered by the trajectory of the robot is approximately 14×2.0 m^2. There was more disturbance in this scenario caused by people passing by and the opening of doors and windows during the run of the experiment. The gas source was placed on the floor in the middle of the investigated corridor segment. Finally, an outdoor scenario was considered. Here, the experiments were carried out in an 8×8 m^2 region that is part of a much bigger open area. Again, the gas source was placed in the middle of this area.

VI. RESULTS

The overlay of the wind information, with the GDM, together with the spatial information of the environment, including source location, provides useful insight into the behaviour and the effect of environmental conditions on the dispersion of the gas. To give a general overview of the data collected, Figure 2 shows the occupancy gridmap of the environment including the gas distribution map obtained in one of the four outdoor experiments (on the left of the figure), the readings of the TGS 2600 sensor during the trial (lower right) and the gas distribution map overlaid with arrows indicating the wind direction. The arrows are coloured according to their relative strength using standard colour coding from blue to red. The gas distribution map was created using the TGS 2600 sensor with a kernel size of 60 cm. In the experiment shown in Figure 2, the maximum of the gas distribution map (indicated by a blue cross) occurred only 36 cm away from the true source location. In Table II a summary of the results obtained from all trials are given, indicating the specified environment, the average wind direction and the approximated distance from the source.

Trial	Wind-X	Wind-Y	Proximity to Source
	Outdoor		
1	(39±93)cm/s	(137±75)cm/s	182 cm
2	(90±79)cm/s	(140±60)cm/s	36 cm
3	(-31±85)cm/s	(87±93)cm/s	23 cm
4	(7±39)cm/s	(36±41)cm/s	254 cm
	Microscope Room		
1	(0.2±4.4)cm/s	(1.6±3.5)cm/s	243 cm
2	(0.5±2.7)cm/s	(1.4±2.5)cm/s	435 cm
3	(0.5±4.0)cm/s	(1.4±3.1)cm/s	202 cm
4	(1.2±10.6)cm/s	(2.4±7.2)cm/s	184 cm
5	(0.6±5.4)cm/s	(2.1±5.6)cm/s	150 cm
6	(-0.7±2.4)cm/s	(0.8±2.2)cm/s	404 cm
	Corridor		
1	(0.5±6.2)cm/s	(0.3±3.1)cm/s	436 cm
2	(5.1±3.0)cm/s	(0.6±2.3)cm/s	785 cm
3	(9.5±5.8)cm/s	(-0.3±4.7)cm/s	269 cm
4	(1.7±6.9)cm/s	(-1.4±5.5)cm/s	234 cm
5	(-1.0±8.5)cm/s	(-0.0±5.3)cm/s	416 cm
6	(5.7±5.5)cm/s	(0.6±6.4)cm/s	308 cm
7	(4.6±9.4)cm/s	(-0.9±6.4)cm/s	258 cm

TABLE II

PARAMETERS SPECIFYING THE GDM EXPERIMENTS.

In examining the outdoor experiments, note that two of the trials showed a close proximity between maximum point of concentration and source location. However, in the two other trials the distance was much larger at 182 cm and 254 cm, respectively. Also note the dominant plume-like structure visible in the gas distribution map in Figure 2 extending to the upper right of the inspected area. This structure is even more pronounced in the gas distribution map created from the more sensitive TGS 2602 gas sensor (map not shown in this paper). As expected, this structure in the gas distribution map appears consistent with the direction of the wind observed and can be explained by the fact that the wind speed and generally the variance of the environmental parameters were much higher than in the indoor experiments.
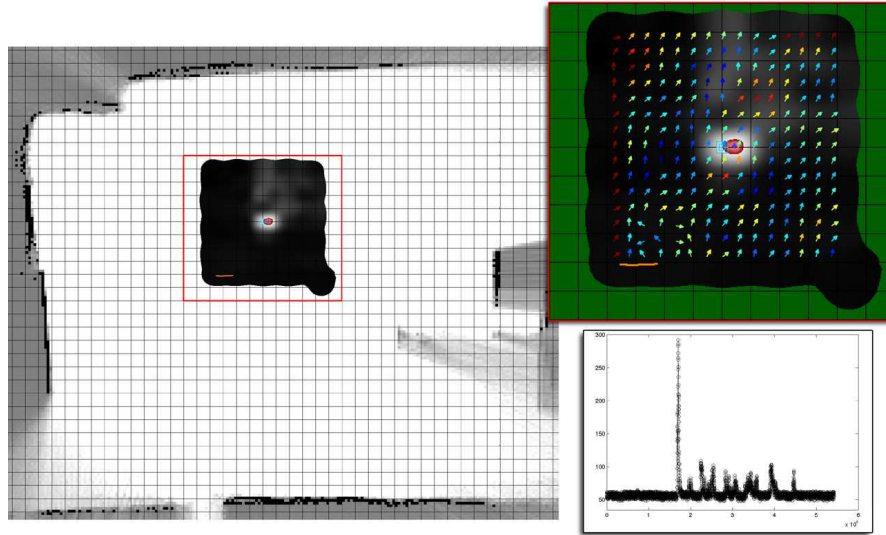
Fig. 2. Left: occupancy gridmap of the outdoor environment including the gas distribution map obtained in one of the four outdoor experiments. The kernel size used was 60 cm. Upper right: the same gas distribution map overlaid with arrows indicating the wind direction. The arrows are coloured according to their relative strength. Lower right: readings of the TGS 2600 sensor versus time (in seconds) during the trial. This sensor was used to create the map.

An example of the results from the enclosed/microscope room are shown in Figure 4. A weaker wind field was observed in this environment compared to the outdoor experiments. Despite the wide passage between the three rooms, the gas concentration was still much lower in the first room (the left room in Figure 4) compared to the other two rooms. Similar results were observed in all the trials. The map in Fig. 4 is a good example of the potential use of an exploration robot acting as an advance guard in a rescue mission. In the case of a poisonous gas, the robot could report that the first room is safe to enter for humans while the other two rooms should be avoided. The division into areas of high and low concentration that appears in the gas distribution map corresponds to the observed airflow field.

Examining the corridor experiments, again a weaker but also relatively uniform and stable wind field was observed. In four out of five trials, this resulted in a division into an area with high and one with low gas concentration. A typical result can be seen in the top panel of Figure 3 where the area of high concentration occurred to the right of the gas source. The maximum of the gas distribution map occurred more than 1.5 m away in all the five trials. This is likely being caused by the lower turbulent intensity that resulted in a slower growth of the plume height, which effectively means that plume tends to reach the gas sensors further downwind. In one particular experiment performed in the corridor, a different distribution was observed where no predominant plume is seen (see second panel in Figure 3, and record 6 in Table II). After further examination of the wind measurements, this was found to correlate with a pronounced change of the environmental conditions. In the first part of the experiment the average wind speed measured while the robot was standing was (-9.5±10.2, -0.6±7.3) cm/s, with z-

component of this vector oriented orthogonal to the floor, i.e. orthogonal to the maps shown in Figure 3. The x- and y-axes in these figures are oriented to the left and upwards as usual. In the second part, the average wind speed was (2.4±4.3, 0.2±4.2) cm/s. At this time also the temperature changes significantly. While the average temperature in the first part was (20.9±0.4)° it increased to (21.7±0.1)° in the second part. The gas distribution maps computed for the first and second part of this experiment are shown in the third and fourth panels in Figure 3. The difference between these two maps is clearly observable. The plume-like structure changed its orientation corresponding to the inversion of the mean wind direction. This particular run of the experiment is interesting as it shows the added utility to overlaying the wind information with the gas distribution map. Not only, does the combination of modalities provide important clues towards gaining insight into the ground truth situation in terms of the spatial propagation of odours, but also can provide instrumental indications about the temporal changes in odour distribution. The combination of temporal and spatial factors are particularly relevant for the majority of pollution monitoring situations.

VII. CONCLUSION AND FUTURE WORK

In this paper we present initial experiments towards environmental monitoring with a mobile platform. A mobile robot was set up as a prototype of a pollution monitoring robot. We describe the design of the robot and the experimental setup and present first monitoring and gas distribution mapping experiments. Next, we discuss the results of altogether 14 trials, which were carried out in three different uncontrolled environments with very different properties: an enclosed indoor area, a part of a long corridor with open
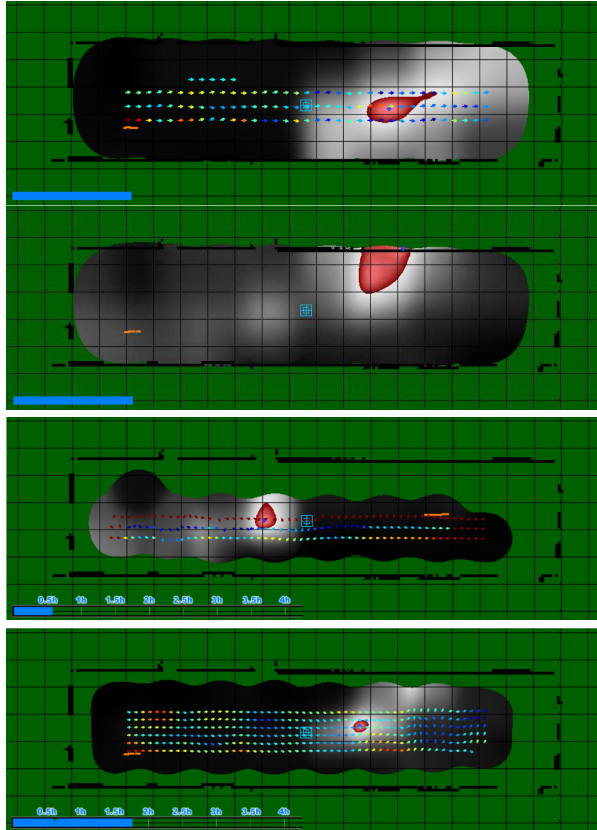
Fig. 3. Gas distribution maps of the corridor experiments overlaid with arrows indicating the wind direction. The first two panels show gas distribution maps obtained in different trials. The third and the forth panels show maps computed from a subset of the measurements from the experiment shown in the second panel. Again, the TGS 2600 gas sensor was used to create the maps and the kernel size was 60 cm.

ends and a high ceiling, and an outdoor scenario. This is an important contribution of this paper since these experiments represent a substantial step towards real world applications.

Many interesting future extensions are feasible with our current setup. One of them would be to implement automatic recognition of the change in the wind direction. The measured data can then be automatically split into subsets so that each subset contains only the measurements made under similar conditions. Mapping will then be more properly done as we saw in Fig. 3. Other sensor modalities, e.g. temperature and humidity sensors can be also used to check if there is an indication of a change in the environment.

A more challenging but also more interesting extension would be to take a closer look at the correlation between the instantaneous gas concentration and wind velocity vector. When the wind direction changed during the sweep over an area, the gas distribution map generated from the measurements typically had multiple peaks distributed over the whole area.
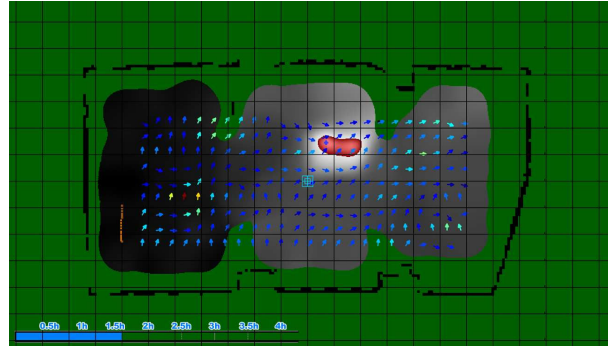

Fig. 4. Gas distribution map of the experiments in the enclosed room overlaid with arrows indicating the wind direction. The TGS 2600 gas sensor was used to create the maps and the kernel size was 60 cm.

REFERENCES

[1] "DustBot - Networked and Cooperating Robots for Urban Hygiene," http://www.dustbot.org.
[2] A. H. Purnamadjaja and R. A. Russell, "Congregation Behaviour in a Robot Swarm Using Pheromone Communication," in *Proc. ACRA*, 2005.
[3] A. Lilienthal, F. Streichert, and A. Zell, "Model-based Shape Analysis of Gas Concentration Gridmaps for Improved Gas Source Localisation," in *Proc. ICRA*, Barcelona, Spain, 2005, pp. 3575 – 3580.
[4] H. Ishida, T. Nakamoto, and T. Moriizumi, "Remote Sensing of Gas/Odor Source Location and Concentration Distribution Using Mobile System," *Sensors and Actuators B*, vol. 49, pp. 52–57, 1998.
[5] P. Pyk, S. Bermúdez Badia, U. Bernardet, P. Knüsel, M. Carlsson, J. Gu, E. Chanie, B. S. Hansson, T. C. Pearce, and P. F. Verschure, "An Artificial Moth: Chemical Source Localization Using a Robot Based Neuronal Model of Moth Optomotor Anemotactic Search," *Auton Robot*, vol. 20, pp. 197–213, 2006.
[6] A. Lilienthal, A. Loutfi, J. L. Blanco, C. Galindo, and J. Gonzalez, "A Rao-Blackwellisation Approach to GDM-SLAM - Integrating SLAM and Gas Distribution Mapping," in *Proc. ECMR*, Freiburg, Germany, 2007, pp. 126–131.
[7] J. Fenger, "Urban Air Quality," *Atmospheric Environment*, vol. 33, pp. 4877–4900, 1999.
[8] Y. Y. Maruo, S. Ogawa, T. Ichino, N. Murao, and M. Uchiyama, "Measurement of Local Variations in Atmospheric Nitrogen Dioxide Levels in Sapporo, Japan, Using a New Method with High Spatial and High Temporal Resolution," *Atmospheric Environment*, vol. 37, pp. 1065–1074, 2003.
[9] P. J. W. Roberts and D. R. Webster, "Turbulent Diffusion," in *Environmental Fluid Mechanics - Theories and Application*, H. Shen, A. Cheng, K.-H. Wang, M. Teng, and C. Liu, Eds. ASCE Press, Reston, Virginia, 2002.
[10] A. Lilienthal and T. Duckett, "Building Gas Concentration Gridmaps with a Mobile Robot," *Robotics and Autonomous Systems*, vol. 48, no. 1, pp. 3–16, August 2004.
[11] A. J. Lilienthal, A. Loutfi, and T. Duckett, "Airborne chemical sensing with mobile robots," *Sensors*, vol. 6, pp. 1616–1678, October 2006.
[12] B. Gerkey, R. T. Vaughan, and A. Howard, "The Player/Stage Project: Tools for Multi-Robot and Distributed Sensor Systems," in *Proc. IEEE ICAR*, 2003, pp. 317–323.
[13] A. Lilienthal and T. Duckett, "Creating Gas Concentration Gridmaps with a Mobile Robot," in *Proc. IROS*, 2003, pp. 118–123.
[14] H. Ishida, A. Kobayashi, T. Nakamoto, and T. Moriizumi, "Three-Dimensional Odor Compass," *IEEE Transactions on Robotics and Automation*, vol. 15, no. 2, pp. 251–257, April 1999.